

Louisiana Tech University

## Louisiana Tech Digital Commons

---

Master's Theses

Graduate School

---

Summer 8-2019

### Design and Analysis of a Traveling Wave Fault Locator

Gerald Austin Taylor

Follow this and additional works at: <https://digitalcommons.latech.edu/theses>



Part of the [Electrical and Computer Engineering Commons](#)

---

**DESIGN AND ANALYSIS OF  
A TRAVELING WAVE  
FAULT LOCATOR**

by

Gerald Austin Taylor, B.S.

A Thesis Presented in Partial Fulfillment  
of the Requirements of the Degree  
Master of Science

COLLEGE OF ENGINEERING AND SCIENCE  
LOUISIANA TECH UNIVERSITY

August 2019

## **ABSTRACT**

The accuracy of fault location is an integral part of power system operations. Improved fault location can reduce maintenance time, increase efficiency, and save money. When a fault occurs, it sends a disturbance in the current and voltage in each direction at almost the speed of light. This disturbance is called a traveling wave, and can be used to locate faults. In efforts to increase accuracy, the use of traveling wave theory to locate faults has become more popular.

This thesis goes through the process of designing and testing a traveling wave fault locator. The design includes analog and digital filtering of the traveling wave signal. The signal passes through an analog high-pass filter that eliminates the fundamental frequency component, an analog low-pass filter that eliminates aliasing, a digital low-pass filter to smooth out the signal, a differentiator to determine the signal's time of arrival, and a peak finder to detect the exact time. Using PSCAD and MATLAB, the traveling wave relay is analyzed with single line-to-ground and line-to-line faults on a power system comparable to the IEEE 9-bus system. The results show that this fault locator is accurate within  $\pm 200$  feet from the fault on a 105-mile line when optimized.

## **APPROVAL FOR SCHOLARLY DISSEMINATION**

The author grants to the Prescott Memorial Library of Louisiana Tech University the right to reproduce, by appropriate methods, upon request, any or all portions of this Thesis. It is understood that “proper request” consists of the agreement, on the part of the requesting party, that said reproduction is for his personal use and that subsequent reproduction will not occur without written approval of the author of this Thesis. Further, any portions of the Thesis used in books, papers, and other works must be appropriately referenced to this Thesis.

Finally, the author of this Thesis reserves the right to publish freely, in the literature, at any time, any or all portions of this Thesis.

Author \_\_\_\_\_

Date \_\_\_\_\_

## TABLE OF CONTENTS

ABSTRACT.....	iii
APPROVAL FOR SCHOLARLY DISSEMINATION .....	iv
LIST OF FIGURES .....	viii
LIST OF TABLES .....	x
ACKNOWLEDGMENTS .....	xi
CHAPTER 1 INTRODUCTION .....	1
1.1    Faults on Transmission Systems.....	1
1.1.1    Single Line-to-Ground Fault.....	1
1.1.2    Double Line-to-Ground Fault .....	2
1.1.3    Three-Phase Fault .....	3
1.1.4    Line-to-Line Fault.....	4
1.2    Traveling Waves .....	5
1.2.1    Reflections .....	5
1.2.2    Velocity of Propagation .....	6
1.2.3    Wave Shapes.....	6
1.2.4    Fault Locating.....	8
1.2.4.1    Double-Ended Method .....	8
1.2.4.2    Single-Ended Method.....	9
1.2.5    Internal and External Faults.....	10
CHAPTER 2 DESIGN PROCESS .....	11
2.1    Generic Design of a Traveling Wave Fault Locator.....	11

2.2	Frequency Spectrum of Traveling Waves .....	12
2.3	Analog Components .....	14
2.3.1	Analog Filtering Process.....	14
2.3.2	Analog High-pass Filter Testing.....	14
2.3.3	Analog Low-pass Filter Testing.....	17
2.3.4	Finalized Analog Components.....	19
2.4	Digital Components .....	19
2.4.1	Digital Filter Design in MATLAB .....	20
2.4.2	Digital Low-pass Filter Design.....	20
2.4.3	Differentiator Design .....	20
2.4.4	Peak Finder .....	21
2.4.5	Digital Component Testing.....	21
2.4.6	Finalized Digital Components .....	22
2.5	Final Traveling Wave Fault Locator Design .....	23
2.6	Limiting Factors.....	24
2.6.1	Instrument Transformers.....	24
2.6.2	Transmission Line Information.....	24
CHAPTER 3 EXPERIMENT SETUP.....		25
3.1	Overview of Test Setup .....	25
3.2	PSCAD.....	25
3.3	Modified IEEE 9-Bus System.....	26
3.3.1	Transmission Lines .....	26
3.3.1.1	Line Parameters .....	27
3.3.1.2	Velocity of Propagation Testing.....	28
3.4	Testing Scenarios .....	29

CHAPTER 4 RESULTS .....	31
4.1    Single Line-to-Ground Fault Results .....	31
4.2    Line-to-Line Fault Results .....	32
CHAPTER 5 DISCUSSION.....	34
CHAPTER 6 CONCLUSIONS AND FUTURE WORK.....	35
6.1    Conclusions.....	35
6.2    Future Work.....	35
APPENDIX A    MATLAB Code of the TWFL.....	37
APPENDIX B    IEEE 9-Bus System Parameters .....	39
BIBLIOGRAPHY .....	41

## LIST OF FIGURES

<b>Figure 1-1:</b> Currents resulting from a SLG fault on phase-A. ....	2
<b>Figure 1-2:</b> Current resulting from a DLG fault on phases A and B. ....	3
<b>Figure 1-3:</b> Current resulting from a 3 $\Phi$ fault. ....	3
<b>Figure 1-4:</b> Current resulting from a LL fault including phases A and B. ....	4
<b>Figure 1-5:</b> Lattice diagram. ....	5
<b>Figure 1-6:</b> Line-to-ground fault wave shape. ....	7
<b>Figure 1-7:</b> LL fault wave shape. ....	7
<b>Figure 1-8:</b> Basic visualization of double-ended traveling wave fault locating. ....	8
<b>Figure 1-9:</b> Basic visualization of single-ended traveling wave fault locating. ....	9
<b>Figure 1-10:</b> Illustration of external fault. ....	10
<b>Figure 2-1:</b> Generic flowchart of the TWFL. ....	12
<b>Figure 2-2:</b> Frequency spectrum of a SLG fault. ....	13
<b>Figure 2-3:</b> Frequency spectrum of a LL fault. ....	13
<b>Figure 2-4:</b> Tower configuration of transmission line for filter testing. ....	15
<b>Figure 2-5:</b> Circuit diagram for the high-pass filter used in final design of the TWFL. .	16
<b>Figure 2-6:</b> Circuit diagram for the low-pass filter used in final design of the TWFL. ..	19
<b>Figure 2-7:</b> Block diagram of analog filtering components. ....	19
<b>Figure 2-8:</b> Screenshot of MATLAB's Filter Design & Analysis Tool. ....	21
<b>Figure 2-9:</b> Finalized digital filtering components. ....	22
<b>Figure 2-10:</b> Flowchart of final TWFL design. ....	23
<b>Figure 3-1:</b> IEEE 9-Bus System for transmission in PSCAD. ....	26



<b>Figure 3-2:</b> Tower configuration for the transmission line connecting buses 4 and 5.....	27
<b>Figure A-1:</b> MATLAB code of the TWFL. ....	37
<b>Figure B-1:</b> Impedance diagram for the IEEE 9-bus system. ....	39
<b>Figure B-2:</b> Load flow diagram for the IEEE 9-bus system. ....	40

## LIST OF TABLES

<b>Table 2-1:</b> Analog High-pass Chebyshev Filter Testing Results.....	16
<b>Table 2-2:</b> Analog Low-pass Chebyshev Filter Testing Results.....	18
<b>Table 2-3:</b> Digital Filtering Component Testing.....	22
<b>Table 3-1:</b> Modified IEEE 9-Bus System Line Parameters. ....	28
<b>Table 3-2:</b> IEEE 9-Bus System Line Parameters. ....	28
<b>Table 3-3:</b> Velocity of Propagation Testing.....	29
<b>Table 3-4:</b> Fault Locations for TWFL testing.....	30
<b>Table 4-1:</b> SLG Fault Results.....	31
<b>Table 4-2:</b> SLG Fault Results (continued). ....	32
<b>Table 4-3:</b> LL Fault Results. ....	33
<b>Table 5-1:</b> Line 6-9, SLG Fault Retest Results.....	34
<b>Table B-1:</b> Generator data for the IEEE 9-bus system.....	40

## **ACKNOWLEDGMENTS**

I would like to acknowledge my major advisor, Dr. Mickey Cox, as well as my committee members, Dr. Prashanna Bhattarai and Dr. Jonathan Walters. Thanks to each of you for the help and guidance over the past few years.

# CHAPTER 1

## INTRODUCTION

### 1.1 Faults on Transmission Systems

In power transmission systems, a fault is any disturbance in the system that can cause changes in current, voltage, power, power factor, impedance, frequency, and temperature. Faults can also cause damage to the transmission line and other equipment. Faults are caused by natural events, such as lightning or fallen trees; physical accidents, such as an automobile crash; equipment failure; and human operating error [1]. Locating these faults is very important to power companies, as improved fault location accuracy can reduce maintenance time, increase efficiency, and save money.

#### 1.1.1 Single Line-to-Ground Fault

The single line-to-ground (SLG) fault occurs when one of the three phases is short circuited to ground. Most of the faults on overhead lines are SLG faults [2]. The currents resulting from a SLG fault on phase-A are shown in **Figure 1-1**. The SLG fault was applied to a 230-kV, 100-mile line with the fault applied 25 miles away. The line's tower configuration is shown in **Figure 2-4**.

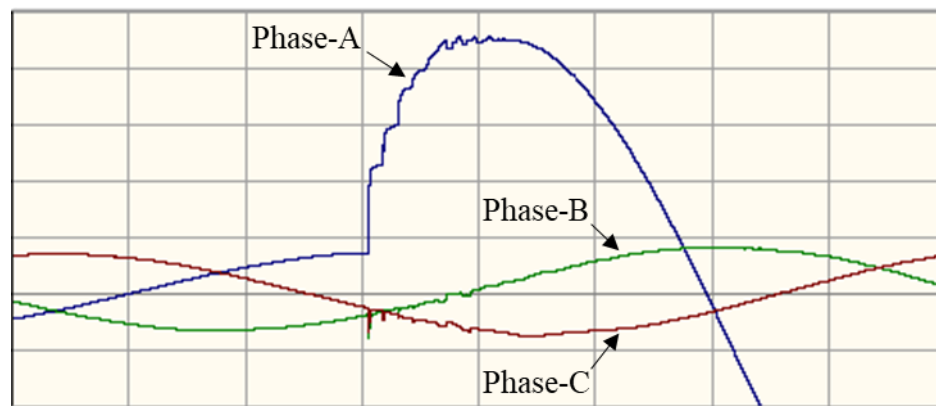


**Figure 1-1:** Currents resulting from a SLG fault on phase-A.

In **Figure 1-1**, the current in phase-A increases to a value of well over four times the maximum current at steady state. The most significant possible change for a line-to-ground happens when the faulted phase is at its maximum value. This is what happens in this case, since the current is at its maximum steady state current. While not as significant of a change, there is noticeable distortion in the other phases when the fault occurs.

#### 1.1.2 Double Line-to-Ground Fault

Similar to the SLG fault, the double line-to-ground (DLG) fault occurs when two of the three phases are short circuited to ground. The currents resulting from a DLG fault on phases A and B are shown in **Figure 1-2**. This fault was applied to the same system as the SLG fault.

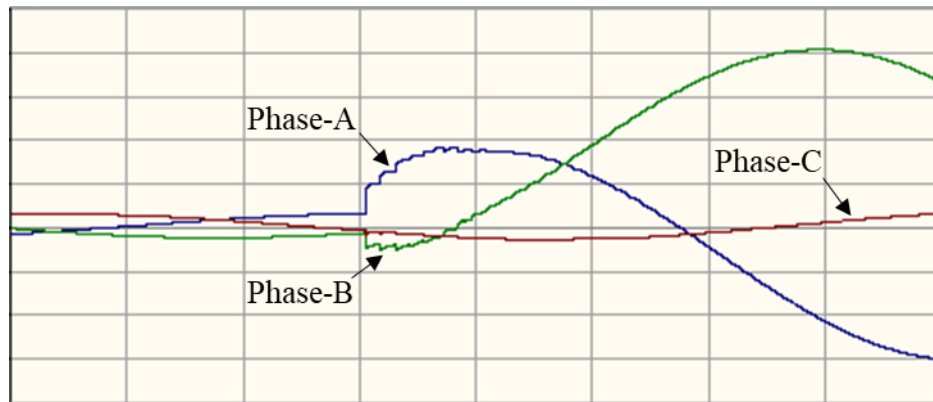


**Figure 1-2:** Current resulting from a DLG fault on phases A and B.

In **Figure 1-2**, phase-A has the exact reaction as in **Figure 1-1**. Phase-B has a similar reaction to phase-A, but it does not make as large of a jump since the current was not at its peak value. It also jumps in the negative direction, because the value of the current at the time of the fault was negative.

### 1.1.3 Three-Phase Fault

Similar to the previous two faults, the three-phase ( $3\Phi$ ) fault occurs when all three phases are short circuited with each other. **Figure 1-3** shows the current resulting from a  $3\Phi$  fault. This fault was applied to the same system as the SLG fault.

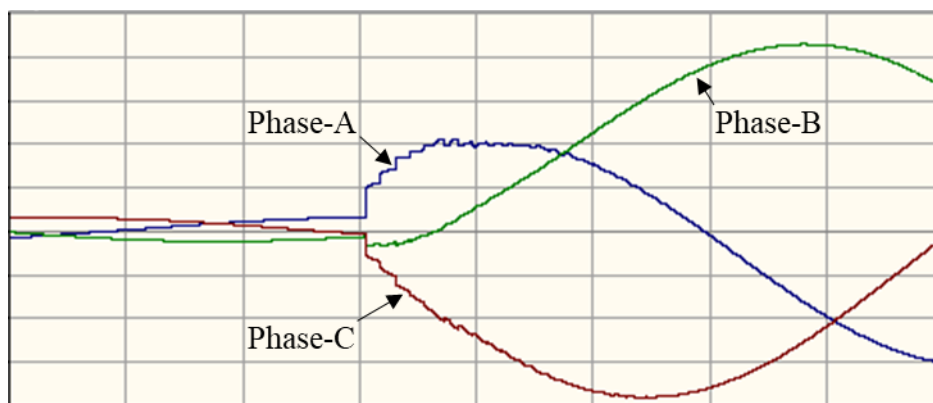


**Figure 1-3:** Current resulting from a  $3\Phi$  fault.

In **Figure 1-3**, phases A and B have the same reaction to the fault as in **Figure 1-2**. Based on phases A and B, phase-C has a predictable reaction, making a large negative jump in current when the fault occurs. Also, the phases do not experience any phase shift when short circuited to ground, and begin to settle into new, larger steady state values after the fault. The sudden jumps in current are the result of that phase attempting to rapidly stabilize to a much larger value, which is shown in all line-to-ground faults.

#### 1.1.4 Line-to-Line Fault

A line-to-line (LL) fault is the result of two phases connecting with each other.

**Figure 1-4** shows the currents resulting from a LL fault with phases A and B faulted.

This fault was applied to the same system as the SLG fault.

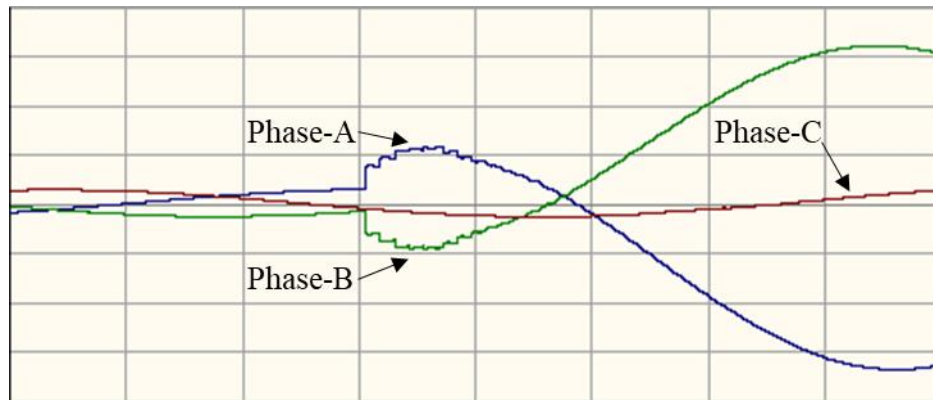


**Figure 1-4:** Current resulting from a LL fault including phases A and B.

**Figure 1-4** show phases A and B having almost identical, but opposite reactions in response to the LL fault. Despite the magnitudes of their respective currents being very different right before the fault, their currents make about the same size jump in opposite directions when the fault occurs. Also, there is a phase shift to where the faulted phases are essentially synchronized, which is the result of the phases actually being connected.

## 1.2 Traveling Waves

When a fault occurs on a transmission line, surges in current and voltage propagate down each end of the line at essentially the speed of light (186,282 mi/s) [3]. This waveform is called a traveling wave and can be used to locate the fault.

### 1.2.1 Reflections

A traveling wave's impact does not end once it reaches the end of the line. The traveling wave will then reflect off of the end of the line and travel in the opposite direction, until it reflects again. Traveling waves reflect off of junctions, which consist of any combination of impedances in series or shunted to ground [4]. Some examples of junctions include transformers, faults, and the line switching from an overhead line to a cable. The behavior of traveling waves after a fault is shown in the lattice diagram in **Figure 1-5**, which is based off the diagram developed by Bewley [4] [5].

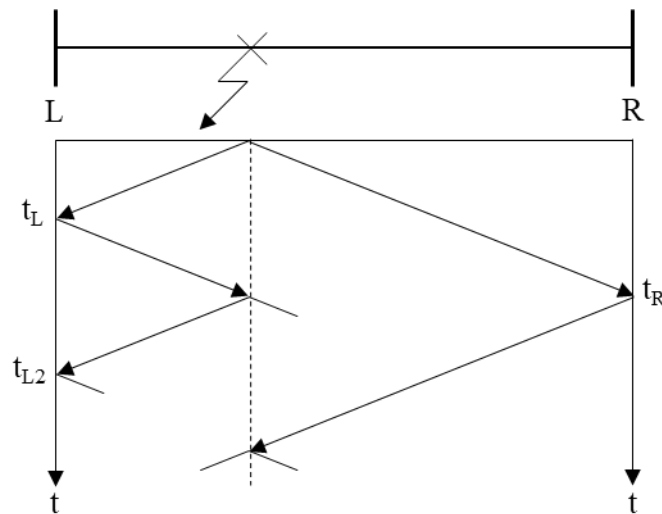


**Figure 1-5:** Lattice Diagram.



### 1.2.2 Velocity of Propagation

An important trait of traveling waves is the speed they travel down transmission lines. This speed is called the velocity of propagation and is unique for each transmission line, since it is based on the line's impedance. Schweitzer Engineering Laboratories, Inc. (SEL) has done extensive work on traveling wave relays and has determined the velocity of propagation in at least two ways. SEL used the inductance and capacitance of a typical 500-kV line to calculate the velocity of propagation as 0.982 times the speed of light (182,929 mi/s) [6]. Later, SEL determined the velocity of propagation using the results of a line energization test on a 161-kV line owned by the Bonneville Power Administration, and found the velocity to be 0.98821 times the speed of light (184,086 mi/s) [7]. For reference, if the velocity of propagation were 184,086 mi/s, it would take a traveling wave 271.6  $\mu$ s to travel 50 mi. At the speed of light, it would take 268.4  $\mu$ s. Since a traveling wave's travel time needs to be specified at such a precise level, these signals must be sampled at high frequencies such as 1 MHz.

### 1.2.3 Wave Shapes

The shapes of traveling waves are also different for each type of fault. While there are multiple types of line-to-ground faults, the wave shapes for each phase are not dependent on other phases. In a line-to-ground fault, the steady state current value of the non-faulted phases remain the same, so looking at one example of a line-to-ground fault will suffice. **Figures 1-6** and **1-7** show the current signals of a faulted phase from a line-to-ground fault and a faulted phase from a line-to-line fault with the fundamental frequency filtered out. The fundamental frequency was filtered out using a 2 kHz Chebyshev high-pass filter.

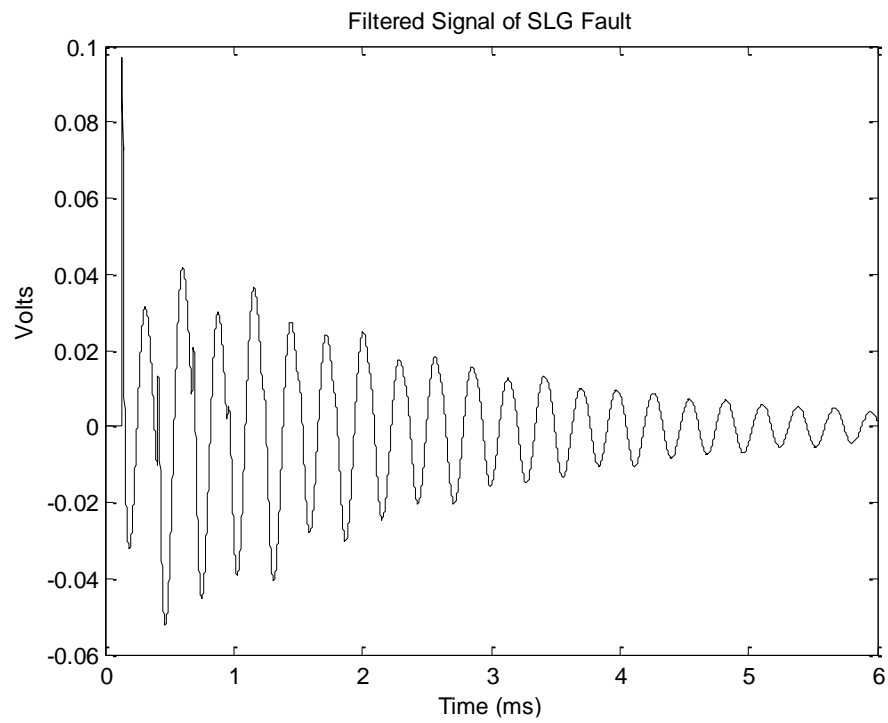


**Figure 1-6:** Line-to-ground fault wave shape.

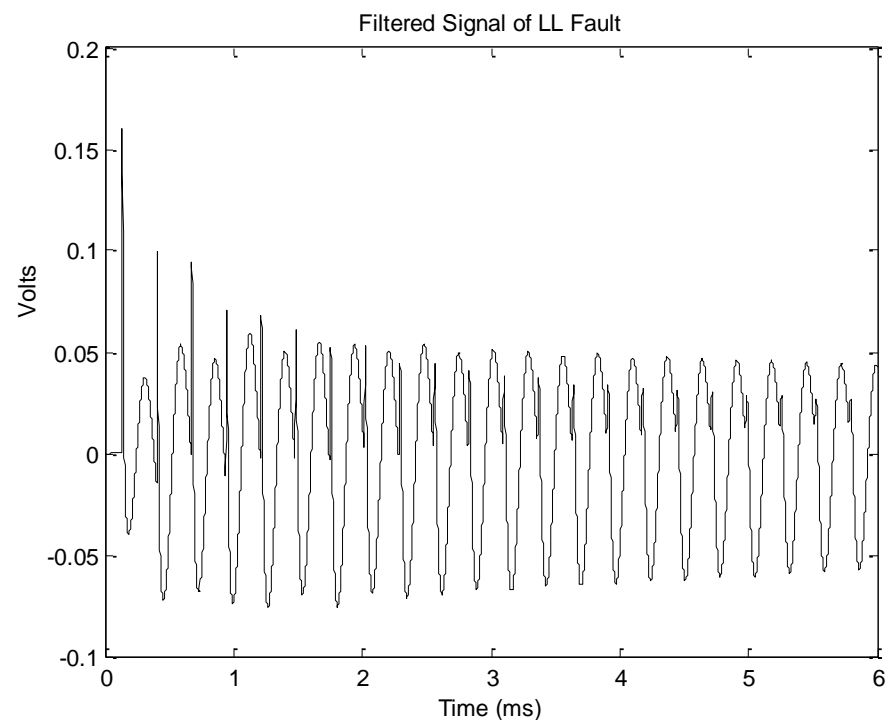


**Figure 1-7:** LL fault wave shape.

### 1.2.4 Fault Locating

Using traveling waves to locate faults is much different from conventional methods. While conventional methods use impedance to locate the fault, traveling wave methods use timing. There are two methods of using traveling waves to locate faults: double-ended and single-ended.

#### 1.2.4.1 Double-Ended Method

The double-ended method records the time of arrival for the traveling wave at each end of the line, and uses the velocity of propagation, the line's length, and the difference in times of arrival to locate the fault. The method also requires communication between the two relays. A visual of the double-ended method is provided in **Figure 1-8**.

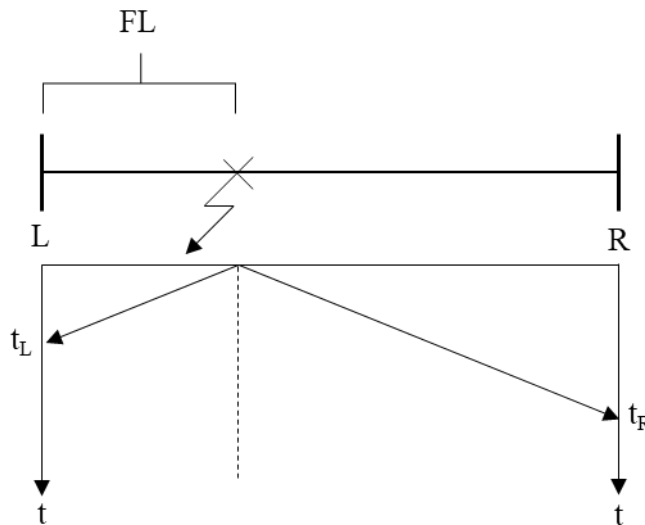


**Figure 1-8:** Basic visualization of double-ended traveling wave fault locating.

The fault location calculation based on the visual above is shown in **Eq. 1-1**.

$$FL = \frac{1}{2} [l_{line} + (t_L - t_R)v_{prop}] \quad \text{Eq. 1-1}$$

For **Eq. 1-1**,  $FL$  is the fault location in miles,  $l_{line}$  is the line length in miles,  $v_{prop}$  is the velocity of propagation in mi/s, and  $t_L$  and  $t_R$  are the times of arrival in seconds for the left and right edges of the line, respectively.

#### 1.2.4.2 Single-Ended Method

The single-ended method also uses the velocity of propagation, but not the line's length. This method is based on the traveling wave's reflections from the lattice diagram in **Figure 1-5**. The line's length is not needed since the fault location can be calculated by using the difference between the fault's time of arrival and the first reflection's time of arrival. A visual of this method is provided in **Figure 1-9**.

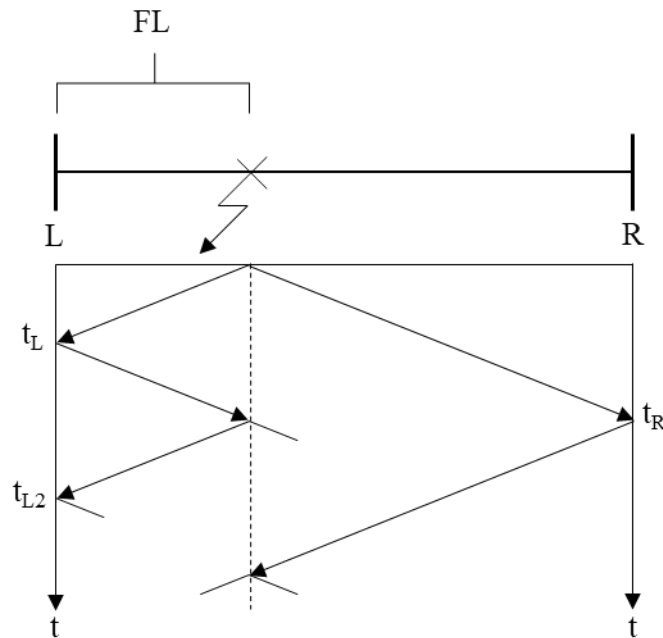


**Figure 1-9:** Basic visualization for single-ended traveling wave fault locating.

The fault location calculation based on the visual above is shown in **Eq. 1-2**.

$$FL = \frac{1}{2} [(t_L - t_{L2})v_{prop}] \quad \text{Eq. 1-2}$$

For **Eq. 1-2**,  $FL$  is the fault location in miles,  $v_{prop}$  is the velocity of propagation in mi/s,  $t_L$  and  $t_R$  is the time of arrival in seconds of the fault at the left edge of the line, and  $t_{L2}$  is the time of arrival of the first reflection.

### 1.2.5 Internal and External Faults

An internal fault is a fault that occurs inside the zone of protection between the relays, and was illustrated in **Figures 1-8** and **1-9**. The single- and double-ended methods for traveling wave fault locating are well prepared for internal faults, but not so much for external faults. External faults happen outside the zone of protection, and send traveling waves that reach the closest relay first. The traveling wave then propagates down the line that the relay was protecting, until it reaches another relay on the opposite side of that line. This should always result in a fault location of either the length of the aforementioned transmission line or zero, depending on which relay is the “left” relay.

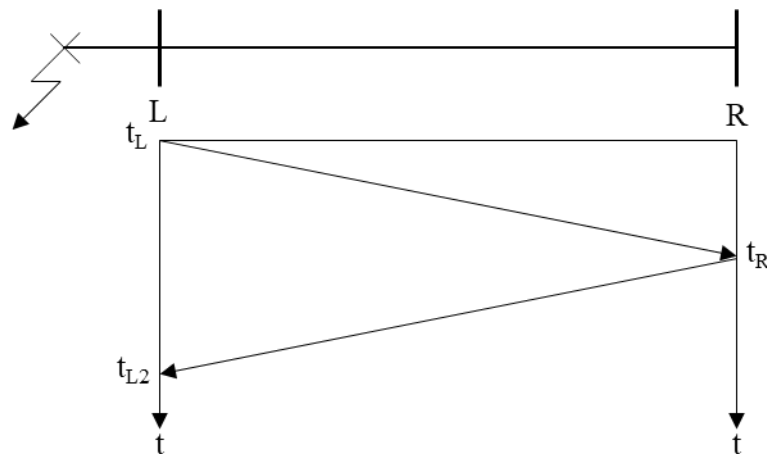


**Figure 1-10:** Illustration of external fault.

## **CHAPTER 2**

### **DESIGN PROCESS**

#### **2.1 Generic Design of a Traveling Wave Fault Locator**

This design will be for a double-ended traveling wave fault locator (TWFL). When a fault occurs, its signal will be received by the TWFLs at the left and right ends after the signal has traveled down the transmission line. In order to analyze the signal received from the fault, it must be processed through filters to determine its time of arrival at the TWFLs on each end. The TWFLs will read the current of the traveling wave, and that current signal will be converted to a voltage signal before the filtering process begins. The traveling wave signal will pass through two analog filters: a high-pass filter to eliminate the 60 Hz component of the transmission line, and a low-pass filter to eliminate aliasing. Then, the signal will pass through two digital filters: a low-pass filter to smooth out the signal, and a differentiator to determine the signal's time of arrival. This is a method SEL used to determine time of arrival [7]. Lastly, a peak finder will estimate the time of arrival for each end, and those times will be put through the fault location equation. The dynamic of the TWFL design is illustrated in the block diagram below.

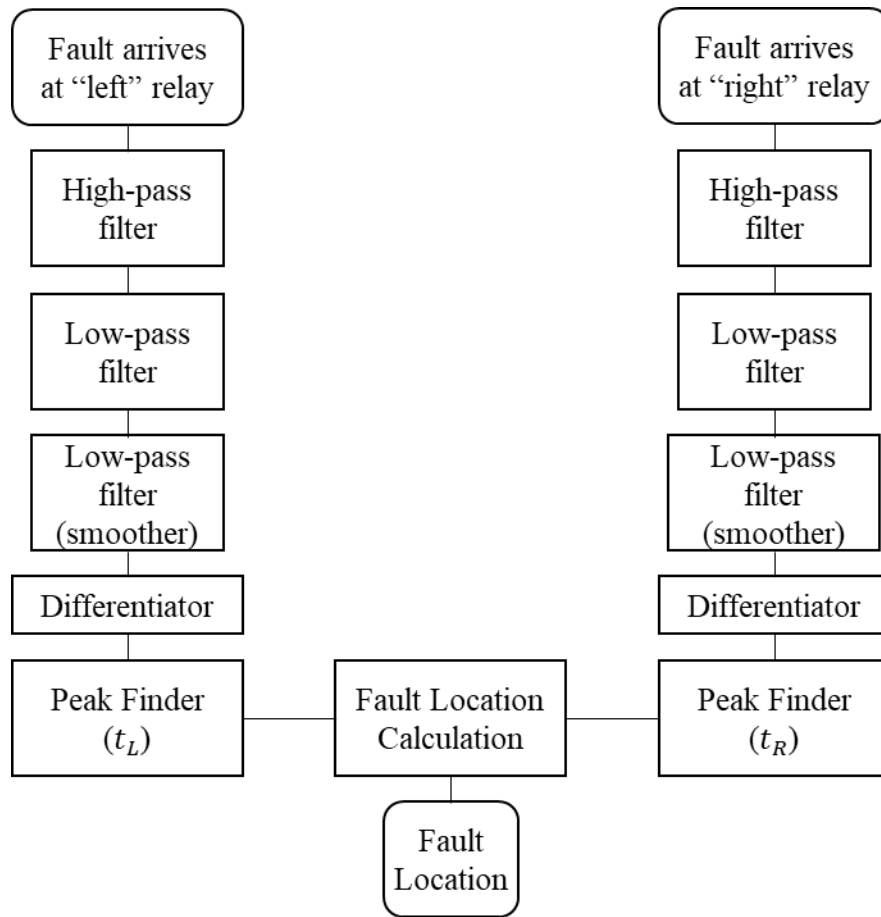


**Figure 2-1:** Generic flowchart of the TWFL.

## 2.2 Frequency Spectrum of Traveling Waves

To select the specifications of the filters in the TWFL, the frequency spectrum of the traveling wave signals must be determined. This was done by performing a Fourier transform on current signals of a SLG fault and a LL fault in MATLAB with the “fft” function. The result of these Fourier transforms are shown in **Figure 2-2** and **Figure 2-3**.

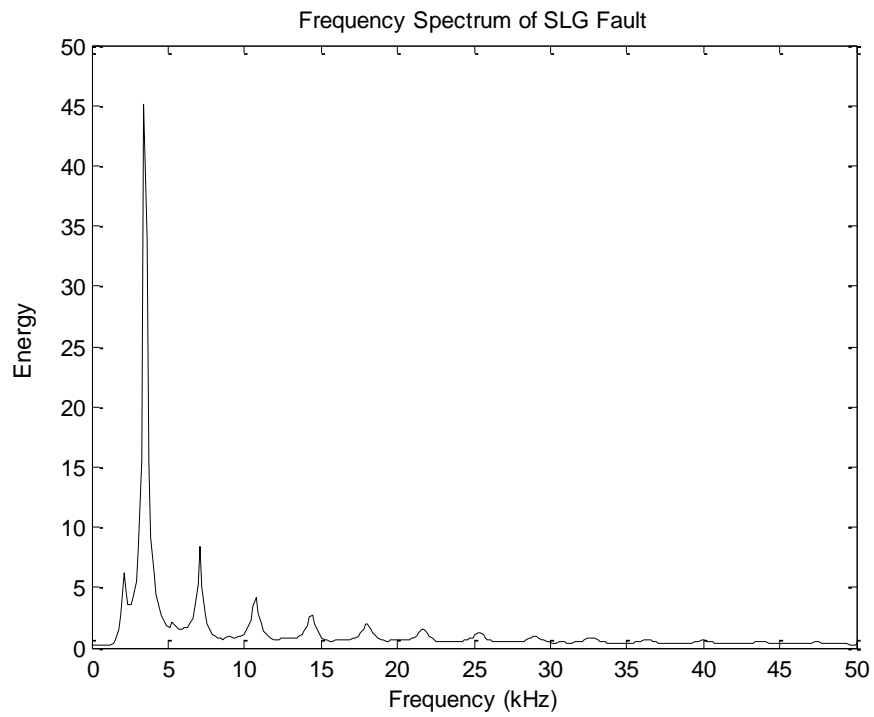


**Figure 2-2:** Frequency spectrum of a SLG fault.

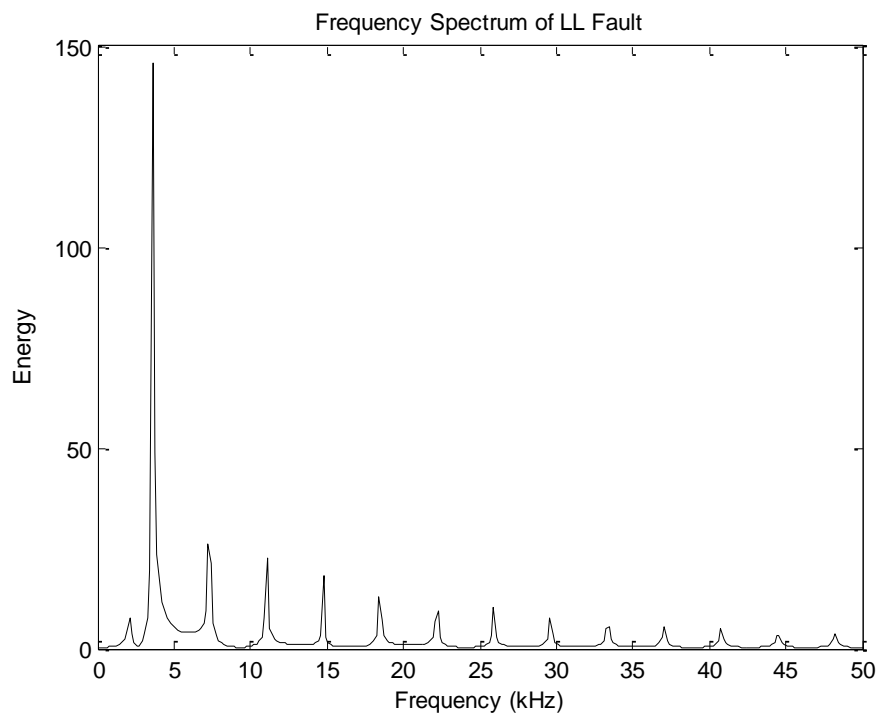


**Figure 2-3:** Frequency spectrum of a LL fault.



Based on the results above, it is clear that the most energy is concentrated around 3.5 kHz for both faults. There is energy at higher frequencies, but it is significantly less than the energy at 3.5 kHz. This implies that the first peak of the signal for both faults has a frequency around 3.5 kHz. For the SLG fault signal, the energy after 20 kHz is essentially negligible, while the same can be said for the LL fault signal after 30 kHz.

## 2.3 Analog Components

### 2.3.1 Analog Filtering Process

The first step in processing the traveling wave signal is passing it through two analog filters. All analog filters in this design will be Chebyshev type, because of its steeper descent from the cutoff frequency to the stopband frequency compared to other filters. Also, in order to guarantee exact high and low cutoff frequencies, this design will consist of a high-pass filter cascaded with a low-pass filter, rather than just a bandpass filter. The filters designed will be constructed in PSCAD.

### 2.3.2 Analog High-pass Filter Testing

The first part of the filtering process is the high-pass filter, which eliminates the 60 Hz component of the power system. Each filter was tested on the same traveling wave signal. This signal was the result of a SLG fault on a 230-kV, 100-mile line with the fault applied 50 miles away. This line's tower configuration is shown in **Figure 2-4**.

The filters were tested based on three criteria: time of the signal's first peak, magnitude of the signal's first peak, and a visual inspection. Since timing is everything with traveling wave fault locating, the first peak time is the most important of the criteria. Almost as important, is the visual inspection, which is solely based on how well the output of the filter represents the inputted signal. Lastly, the first peak magnitude will

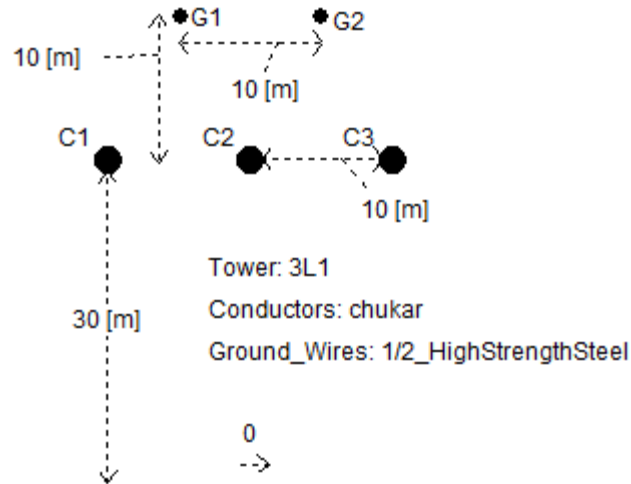


**Figure 2-4:** Tower configuration of transmission line for filter testing.

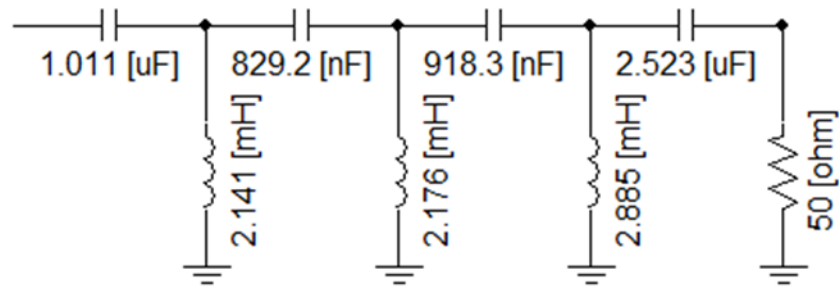
Help evaluate the efficiency of the filter and the relationship between the magnitude and the order. The actual magnitudes were scaled to a range of 0 to 10 for simplicity.

In order to eliminate the 60 Hz component, filters with cutoff frequencies of 500 Hz, 1 kHz, and 2 kHz were tested. At these cutoff frequencies, ripples of 0.1 dB and 0.5 dB, as well as orders of 3 through 7 were all tested. All of the results, except for the visual inspection, are in **Table 2-1**.

The filters with cutoff frequency of 500 Hz were so ineffective that measurements could not be taken, so those results are not included in the table above. Based on the results, the 2 kHz, 7<sup>th</sup>-order filter with 0.1 dB ripple was selected for the design. The circuit diagram of this filter is shown in **Figure 2-5**.

**Table 2-1:** Analog High-pass Chebyshev Filter Testing Results.

$F_c$ (kHz)	Ripple (dB)	Order	1 <sup>st</sup> Peak Time ( $\mu$ s)	1 <sup>st</sup> Peak Magnitude
1	0.1	3	285.0	10.00
		4	280.9	8.80
		5	272.4	8.58
		6	271.9	8.49
		7	271.5	8.45
	0.5	3	284.3	9.61
		4	280.7	8.81
		5	272.1	8.52
		6	271.4	8.20
		7	271.4	8.20
2	0.1	3	272.2	8.56
		4	271.5	8.30
		5	271.1	8.06
		6	270.8	7.88
		7	270.6	7.67
	0.5	3	271.9	8.47
		4	271.5	8.30
		5	270.9	7.95
		6	270.9	7.95
		7	270.5	7.57

**Figure 2-5:** Circuit diagram for the high-pass filter used in final design of the TWFL.

### 2.3.3 Analog Low-pass Filter Testing

The second part of the filtering process is the low-pass filter, which eliminates aliasing. These filters were tested on the same system and with the same criteria as the high-pass filters in the previous sub-section. Filters with cutoff frequencies of 500 kHz, 600 kHz, and 700 kHz were tested. At these cutoff frequencies, ripples of 0.1 dB and 0.5 dB, as well as orders of 3 through 7 were all tested. All of the results, except for the visual inspection, are in **Table 2-2**.

Based on the results in **Table 2-2**, the 500 kHz, 3<sup>rd</sup>-order filter with 0.1 dB ripple was selected for the design. Though it seems like the 600 kHz filters performed better, they did not represent the original traveling wave signal as well as the 500 kHz filters. The circuit diagram of this filter is shown in **Figure 2-6**.

**Table 2-2:** Analog Low-pass Chebyshev Filter Testing Results.

$F_c$ (kHz)	Ripple (dB)	Order	1 <sup>st</sup> Peak Time ( $\mu$ s)	1 <sup>st</sup> Peak Magnitude
500	0.1	3	270.7	9.39
		4	270.9	9.68
		5	271.2	9.74
		6	271.6	9.99
		7	271.9	10.00
	0.5	3	270.7	9.25
		4	271.0	9.96
		5	271.3	9.59
		7	272.0	9.82
		600	0.1	3
4	270.6			9.41
5	270.9			9.46
6	271.1			9.71
7	271.4			9.72
0.5	3		270.4	8.99
	4		270.6	9.67
	5		270.9	9.32
	7		271.5	9.56
	700		0.1	3
4		271.7		9.43
5		271.9		9.42
6		272.2		9.56
7		272.5		9.51
0.5		3	271.6	9.35
		4	271.7	9.55
		5	272.0	9.32
		7	272.6	9.35

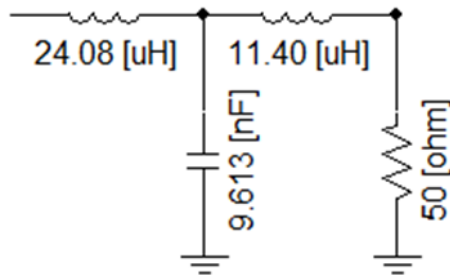


**Figure 2-6:** Circuit diagram for the low-pass filter used in final design of the TWFL.

#### 2.3.4 Finalized Analog Components

The final design will contain the 2 kHz, 7<sup>th</sup>-order high-pass filter with 0.1 dB ripple cascaded with the 500 kHz, 3<sup>rd</sup>-order low-pass filter with 0.1 dB ripple. Once the traveling wave signal passes through the analog filtering process, it will then be converted to a digital signal, where the digital filtering process begins.

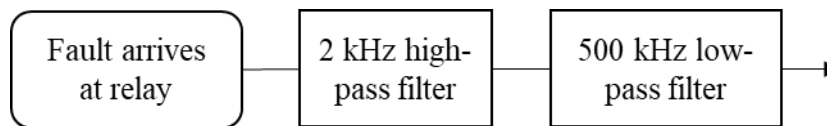


**Figure 2-7:** Block diagram of analog filtering components.

## 2.4 Digital Components

After the analog filtering process, the signal is converted to a digital signal. This is done by transferring the signal from PSCAD to MATLAB. Once the signal is in MATLAB, it begins the digital filtering process. This process begins with a Chebyshev low-pass filter used to smooth out the traveling wave signal and remove unwanted noise and distortion. Then, the signal goes through a differentiator, which will help determine the signal's time of arrival. To estimate the signal's time of arrival, it will then be evaluated by a peak finder, which pinpoints the time that the signal arrives. Once the time

of arrival is determined for the left and right traveling wave signals, those times will be inserted into **Eq. 1-1**, where the location of the fault will be calculated.

#### 2.4.1 Digital Filter Design in MATLAB

Designing filters in MATLAB is relatively simple. There are multiple ways to design filters in MATLAB, but the process used in this design is accessing the Filter Design and Analysis Tool. This is done by typing “fdatool” in MATLAB’s Command Window. In the Filter Design and Analysis Tool, the user enters all the specifications of their filter, and lets the tool itself design it for them. After the design is finished, the tool is able to convert that design to MATLAB code, which can be used in any MATLAB scripts.

#### 2.4.2 Digital Low-pass Filter Design

The digital filters chosen for this design are all Chebyshev Type II filters, for the same reasons stated in section 2.3.1. The filters designed and tested will have cutoff frequencies of 20, 25, and 30 kHz. They will also have stopband frequencies of +5, +10, +15, and +20 kHz of the cutoff frequencies. All filters will have an attenuation of 50 dB with a ripple of 0.1 dB.

#### 2.4.3 Differentiator Design

The differentiator will be directly related to the analog high-pass filter and the digital low-pass filter. Part of the differentiator design is the frequency vector  $[f_1 f_2 f_3 f_4]$ . For the differentiator of this design,  $f_1$  is 0,  $f_2$  is the cutoff frequency of the analog high-pass filter,  $f_3$  is the cutoff frequency of the digital low-pass filter, and  $f_4$  is 500 kHz.

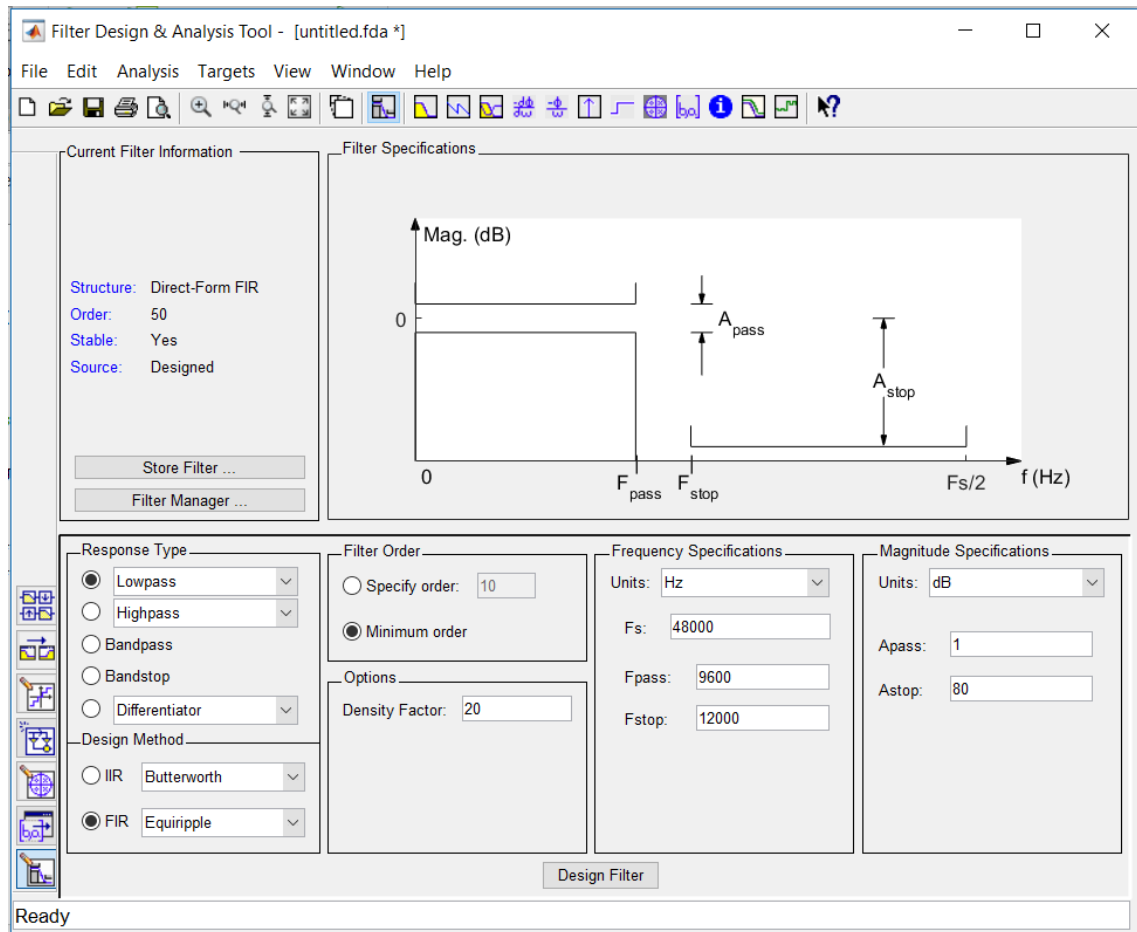


**Figure 2-8:** Screenshot of MATLAB's Filter Design & Analysis Tool.

#### 2.4.4 Peak Finder

The peak finder is final step of the filtering process. To find the exact first peak of the signal, MATLAB's "findpeaks" function is used. This function returns the value and location of each peak. The location of the first peak is used as the time of arrival for that signal, which is then used in the fault location equation.

#### 2.4.5 Digital Component Testing

All digital components are tested on the same system as the analog components, except the fault will be applied at 25 miles. Since the TWFL is technically complete at this point, the performance of these filters is based solely on fault location accuracy.



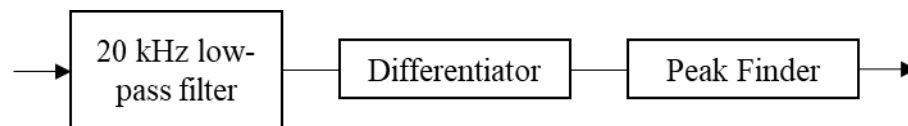
**Table 2-3:** Digital Filtering Component Testing.

$F_c$ (kHz)	$f_s$ (kHz)	Order	Fault Location Error (ft)
20	25	12	147
	30	9	98
	35	8	147
	40	7	147
25	30	14	147
	35	10	147
	40	8	98
	45	7	98
30	35	15	147
	40	11	147
	45	9	147
	50	8	147

Based on the results above, the 20 kHz, 9<sup>th</sup>-order low-pass Chebyshev filter with a stopband frequency of 30 kHz was chosen. This was chosen above the similar 25 kHz filters because of its lower cutoff frequency.

#### 2.4.6 Finalized Digital Components

The final design will consist of a 20 kHz, 9<sup>th</sup>-order low-pass Chebyshev filter with a stopband frequency of 30 kHz, a differentiator with frequency vector of [0 2 20 500] kHz, and a peak finder using MATLAB's "findpeaks" function.

**Figure 2-9:** Finalized digital filtering components.

## 2.5 Final Traveling Wave Fault Locator Design

The flowchart in **Figure 2-10** represents the complete and final design of the TWFL. The MATLAB code for the digital filtering and fault location calculation is shown in Appendix A. This design will be tested in multiple ways to evaluate its accuracy.

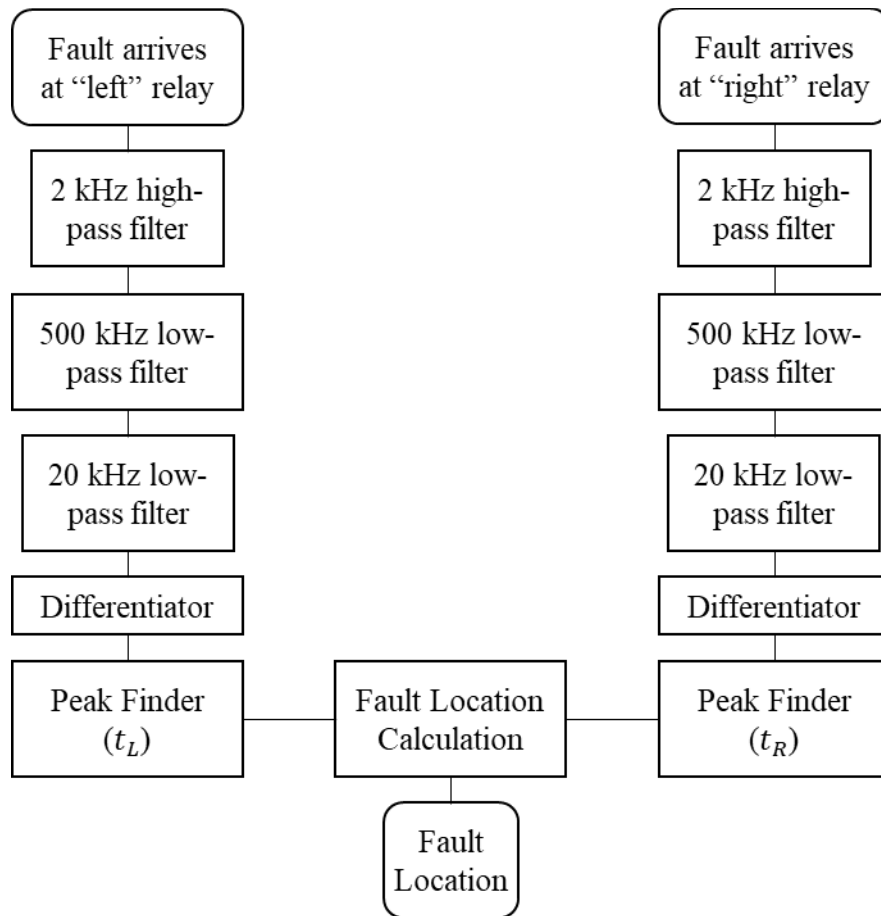


**Figure 2-10:** Flowchart of final TWFL design.

## 2.6 Limiting Factors

### 2.6.1 Instrument Transformers

The entire fault location process for the TWFL is dependent on the signals from the traveling wave. The accuracy of the standard instrument transformers is vital to the accuracy of the TWFL. SEL performed studies that showed conventional CTs were accurate enough at high frequencies to use for traveling waves, but commonly used capacitance coupled voltage transformers (CCVTs) did not properly measure the traveling wave transients [8].

### 2.6.2 Transmission Line Information

Finding the transmission line's exact parameters is an important factor in locating faults. In the case of TWFLs, at least the line length and velocity of propagation are needed. The distance a line covers may be known, but not knowing the additional line length due to sag will make the TWFL less accurate. Also, a line's tower configuration may not be uniform throughout, so calculating the velocity of propagation can be very tedious. It is much more efficient to perform a test like SEL did on one of the Bonneville Power Administration's lines, where they used the results of a line energization test [7].

## **CHAPTER 3**

### **EXPERIMENT SETUP**

#### **3.1 Overview of Test Setup**

The TWFL will be tested in many different ways on one system. In order to obtain results on a realistic system, the IEEE 9-bus system for load flow was chosen for testing. The TWFL will be tested with two different faults at five locations on all six of the system's transmission lines. The two faults applied will be a SLG fault and a LL fault. The SLG fault was chosen since it is the most common fault, and the LL fault was chosen because its waveform is the most different from the SLG fault. These faults will be applied at distances of 10%, 30%, 50%, 70%, and 90% of the transmission line's length from the left edge of the line. All of these faults will be applied to the system in PSCAD.

#### **3.2 PSCAD**

Power Systems Computer Aided Design (PSCAD) is the simulation software that was used for these experiments. PSCAD allows the user to construct circuits, run simulations, and analyze results in one interface. The engine behind PSCAD is EMTDC (Electromagnetic Transients including DC), which is a simulation tool capable of duplicating the responses of power systems at all frequencies. This is very important for evaluating traveling waves, which materialize far outside fundamental frequency of electrical power systems.

### 3.3 Modified IEEE 9-Bus System

The system used for these tests is a modified version of the IEEE 9-bus system for transmission. This was chosen because it provided a small, yet accurate system for fault studies. This system consists of nine buses, three generators, three loads, three transformers, and six transmission lines. Also, it has a base voltage of 230 kV, and a base power of 100 MVA. Parameters for the IEEE 9-bus system are located in Appendix B.

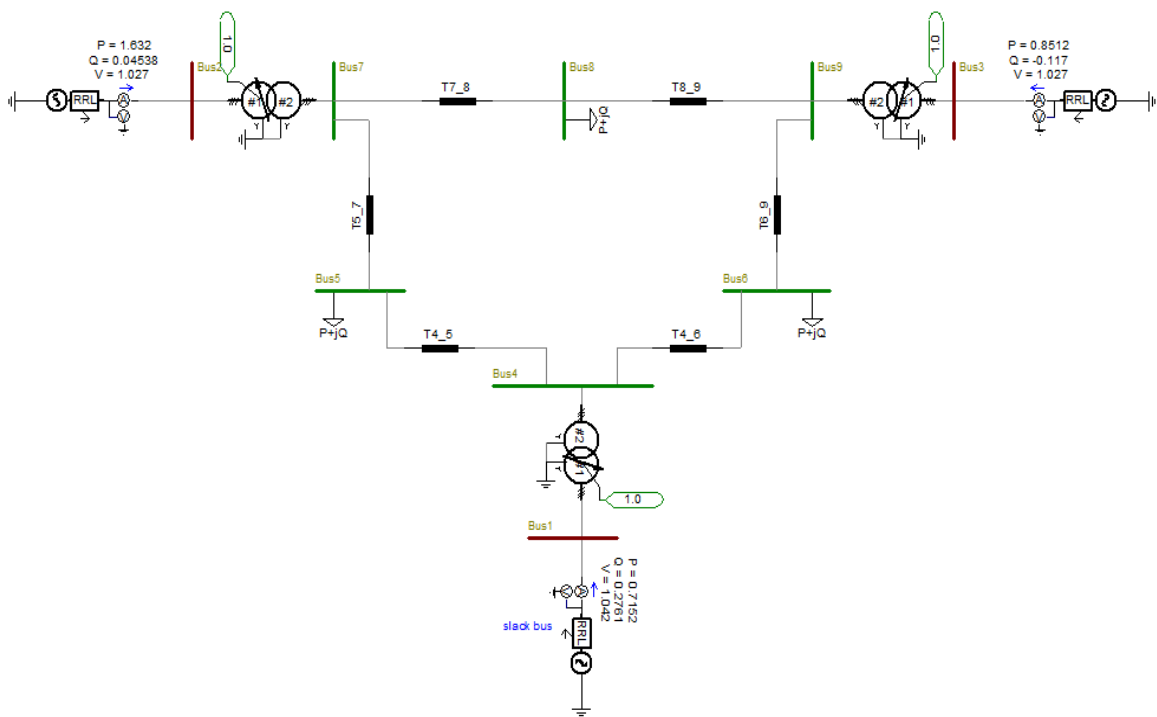


**Figure 3-1:** IEEE 9-Bus System for transmission in PSCAD.

#### 3.3.1 Transmission Lines

The one difference between the IEEE 9-bus system and the system used for these experiments, are the transmission lines. Normally, transmission lines for these types of systems are modelled using the Bergeron line model. The Bergeron model is effective for most simulations, but it calculates all parameters at only one frequency, which is usually the fundamental frequency. For this case, the transmission lines were modelled using the

frequency dependent (phase) model, which is accurate for all frequencies and transmission configurations [9]. Transmission lines modelled by the frequency dependent (phase) model must be designed by using the tower configuration, whereas lines modelled by the Bergeron model can be designed by just using the line parameters. This issue caused the line parameters for the system used for testing to be different than the official IEEE 9-bus system, since the line parameters for the IEEE 9-bus system cannot be recreated using a reasonable tower configuration.

### 3.3.1.1 Line Parameters

In order to use the frequency dependent (phase) model, all lines on the system were redesigned. A generic three-phase flat tower configuration was used for all lines, and the line lengths and ACSR conductors were adjusted to obtain the IEEE 9-bus system's resistance values and a range of line length's ideal for fault location testing. For **Table 3-1** and **Table 3-2**, the line numbers are represented by the buses they connect.

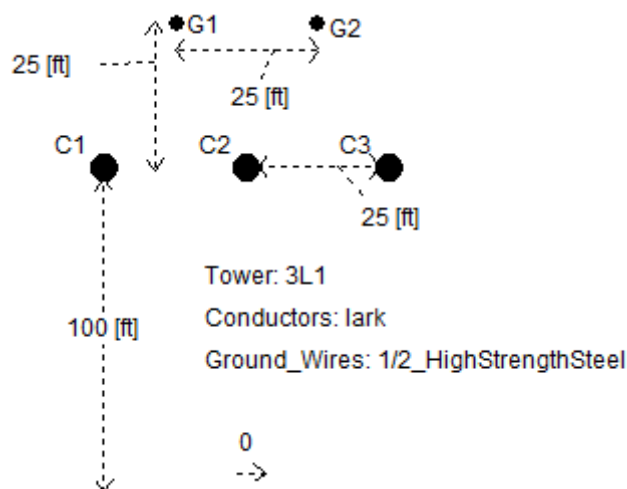


**Figure 3-2:** Tower configuration for the transmission line connecting buses 4 and 5.

**Table 3-1:** Modified IEEE 9-Bus System Line Parameters.

Line	Length [mi]	ACSR Conductor	R [ $\Omega$ ]	X [ $\Omega$ ]	B [S]
4-5	22.51	Lark	5.29	19.21	9007
4-6	45.87	Hawk	8.99	38.91	4380
5-7	72.04	Lark	16.93	61.48	2814
6-9	105.26	Hawk	20.63	89.28	1390
7-8	14.47	Ostrich	4.50	12.68	1847
8-9	32.14	Hawk	6.30	27.26	4243

**Table 3-2:** IEEE 9-Bus System Line Parameters.

Line	R [ $\Omega$ ]	X [ $\Omega$ ]	B [S]
4-5	5.29	35.97	3006
4-6	8.99	48.67	3348
5-7	16.93	85.17	1729
6-9	20.63	91.94	1448
7-8	4.50	30.47	3550
8-9	6.30	53.32	2531

### 3.3.1.2 Velocity of Propagation Testing

In order to get the most accurate fault location estimation, the velocity of propagation must be determined. Since the testing will take place on a system with six transmission lines, the velocity of propagation will be determined for each line, and the average of those values will be used for fault location on the entire system. To determine the velocity of propagation, a  $3\Phi$  fault will be applied at one end of the line, and the time of arrival at the opposite end of the line will be recorded. That value and the line's length will determine the line's velocity of propagation. A  $3\Phi$  fault was chosen so that the time

of arrival could be checked for all three phases. **Table 3-3** shows that the average velocity of propagation for the system is 185,433 mi/s, or 0.99544 times the speed of light.

**Table 3-3:** Velocity of Propagation Testing.

Line	Line Length (mi)	Travel Time ( $\mu$ s)	Velocity of Propagation (mi/s)
4-5	22.51	121.5	185,267
4-6	45.87	247.6	185,258
5-7	72.04	388.9	185,240
6-9	105.26	566.7	185,742
7-8	14.47	78.04	185,418
8-9	32.14	173.1	185,673

Average Velocity of Propagation = 185,433 mi/s

### 3.4 Testing Scenarios

In order to gauge the effectiveness of the TWFL, it must be tested in many different scenarios. The TWFL will be tested by two different faults at five locations on the six lines in the modified IEEE 9-bus system. The two faults chosen for testing are the SLG fault and the LL fault. These were chosen because of their difference in wave shapes. These faults will be applied at five locations, which will be related to the transmission line's length. These five locations are 10%, 30%, 50%, 70%, and 90% of the line's length from the left edge of the line, and are specified in **Table 3-4**. A total of sixty tests were run to evaluate the performance of the TWFL.



**Table 3-4:** Fault Locations for TWFL testing.

Line	Line Length (mi)	Fault Location	Actual Fault Location (mi)
4.5	22.51	10%	2.25
		30%	6.75
		50%	11.26
		70%	15.76
		90%	20.26
4.6	45.87	10%	4.59
		30%	13.76
		50%	22.94
		70%	32.11
		90%	41.28
5.7	72.04	10%	7.20
		30%	21.61
		50%	36.02
		70%	50.43
		90%	64.84
6.9	105.26	10%	10.53
		30%	31.58
		50%	52.63
		70%	73.68
		90%	94.73
7.8	14.47	10%	1.45
		30%	4.34
		50%	7.24
		70%	10.13
		90%	13.02
8.9	32.14	10%	3.21
		30%	9.64
		50%	16.07
		70%	22.50
		90%	28.93

## CHAPTER 4

### RESULTS

#### 4.1 Single Line-to-Ground Fault Results

The following results are for the SLG fault testing. For **Table 4-1**, the fault location values are the distances from the left edge of the transmission line.

**Table 4-1:** SLG Fault Results.

Line	Length (mi)	Actual Fault Location (mi)	Estimated Fault Location (mi)	Error (ft)
4-5	22.51	2.25	2.2803	160
		6.75	6.7584	44
		11.26	11.2643	23
		15.76	15.7516	-44
		20.26	20.2297	-160
4-6	45.87	4.59	4.5777	-65
		13.76	13.7564	-19
		22.94	22.9350	-26
		32.11	32.1136	19
		41.28	41.2923	65
5-7	72.04	7.20	7.1861	-73
		21.61	21.6494	208
		36.02	36.0200	0
		50.43	50.3906	-208
		64.84	64.8539	73

**Table 4-2:** SLG Fault Results (continued).

Line	Length (mi)	Actual Fault Location (mi)	Estimated Fault Location (mi)	Error (ft)
6-9	105.26	10.53	10.6308	532
		31.58	31.6483	361
		52.63	52.6300	0
		73.68	73.6117	-361
		94.73	94.6292	-532
7-8	14.47	1.45	1.4497	-2
		4.34	4.3423	12
		7.24	7.2443	23
		10.13	10.1277	-12
		13.02	13.0111	-47
8-9	32.14	3.21	3.2477	199
		9.64	9.6728	173
		16.07	16.0700	0
		22.50	22.4672	-173
		28.93	28.8923	-199

#### 4.2 Line-to-Line Fault Results

The following results are for the line-to-line fault testing. For **Table 4-2**, the fault location values are the distances from the left edge of the transmission line.

**Table 4-3: LL Fault Results.**

Line	Length (mi)	Actual Fault Location (mi)	Estimated Fault Location (mi)	Error (ft)
4-5	22.51	2.25	2.2618	62
		6.75	6.7677	93
		11.26	11.2550	-26
		15.76	15.7423	-93
		20.26	20.2482	-62
4-6	45.87	4.59	4.5777	-65
		13.76	13.7564	-19
		22.94	22.9350	-26
		32.11	32.1136	19
		41.28	41.2923	65
5-7	72.04	7.20	7.1861	-73
		21.61	21.6494	208
		36.02	36.0200	0
		50.43	50.3906	-208
		64.84	64.8539	73
6-9	105.26	10.53	10.5381	43
		31.58	31.6483	361
		52.63	52.6300	0
		73.68	73.6117	-361
		94.73	94.7219	-43
7-8	14.47	1.45	1.4682	96
		4.34	4.3423	12
		7.24	7.2350	-26
		10.13	10.1277	-12
		13.02	13.0018	-96
8-9	32.14	3.21	3.2570	248
		9.64	9.6542	75
		16.07	16.0700	0
		22.50	22.4858	-75
		28.93	28.8830	-248

## CHAPTER 5

### DISCUSSION

Overall, the TWFL performed very well, only allowing two cases where the estimated fault location exceeded  $\pm 400$  feet error, which took place on line 6-9. Lines 4-6 and 7-8 were the most accurate, with every estimated fault location within 100 feet of the actual fault location. Lines 6-9 and 8-9 were the least accurate, which is the result of the velocity of propagation. **Table 3-3** shows that the velocities of propagation for lines 6-9 and 8-9 were the furthest off of the average velocity of propagation used for testing. The worst case were the SLG faults on line 6-9, and were retested using the line's actual velocity of propagation, 185,742 mi/s.

**Table 5-1:** Line 6-9, SLG Fault Retest Results.

Length (mi)	Actual Fault Location (mi)	Estimated Fault Location (mi)	Error (ft)
105.26	10.53	10.5632	175
	31.58	31.6133	176
	52.63	52.6300	0
	73.68	73.6467	-176
	94.73	94.6968	-175

These results show significant improvement with an accuracy within  $\pm 200$  feet of the fault on the 105.26-mile line.

## **CHAPTER 6**

### **CONCLUSIONS AND FUTURE WORK**

#### **6.1 Conclusions**

Using traveling waves is a very effective way to locate faults. The performance of TWFLs is dependent on the instrument transformers, transmission line parameters, velocity of propagation, and fault characteristics. When these are optimized, the TWFL designed in this paper is accurate to within  $\pm 200$  feet of the fault on lines up to 105 miles long. Accurate fault locations can save power companies money by reducing maintenance time and increasing efficiency.

The velocity of propagation is a very important component of traveling wave fault locating. Changing the velocity by just 309 mi/s resulted in a drastic change in fault location accuracy on line 6-9, reducing the errors from  $\pm 532$  and  $\pm 361$  feet to  $\pm 175$  and  $\pm 176$  feet, respectively. This TWFL is more accurate when only taking one line and its respective velocity of propagation into consideration, rather than accounting for and adjusting to the entire system.

#### **6.2 Future Work**

There is plenty of future work that could be done on this TWFL project. Enhancing communications between the TWFLs and adding a velocity of propagation database would account for the possible velocity errors. When a fault occurs, the first two

relays intercepting the traveling waves would determine which line is faulted, then access the database to determine which velocity of propagation value to use in the fault location equation. This would be effective for TWFLs protecting multiple lines.

More future work would be building on this TWFL to make it a full traveling wave relay. This would include adding features such as deciding whether or not to trip a breaker, determining the type of fault (SLG, LL, etc.), and determining the direction of the fault (internal or external).

Despite some studies, it is not fully known which instrument transformers have a frequency response reliable enough to work with traveling wave relays. More tests and investigations could be done to clarify the frequency response and reliability of conventional transformers.

## APPENDIX A

### MATLAB CODE OF THE TWFL

Shown in **Figure A-1** is the MATLAB code containing the digital components of the TWFL. These components are the 20 kHz low-pass filter (smoother), differentiator, peak finder, and fault location calculation.

```
1 function [fl] = TWFL(LL,Vprop,sigL,sigR)
2 % This function is locating faults using traveling waves
3 % input:
4 %   twfl(LL,Vprop,sigL,sigR)
5 %   LL = line length (mi)
6 %   Vprop = velocity of propagation (mi/s)
7 %   sigL = traveling wave signal vector of left edge of line
8 %         (sampled every 1 MHz)
9 %   sigR = traveling wave signal vector of right edge of line
10 %        (sampled every 1 MHz)
11 %        (sigL and sigR must start and end at the same time)
12 % output:
13 %   [fl]
14 %   fl = fault location (mi)
15
16 % magnify signal from analog filters
17 L_HPLP = sigL*100;
18 R_HPLP = sigR*100;
19
20 % construction of low-pass filter (smoother)
21 l = fdesign.lowpass(20,30,0.1,50,1000);
22 LPF = design(l, 'cheby2', 'MatchExactly', 'stopband');
23
24 % traveling wave signal leaving low-pass filter
25 L_LPF = filter(LPF,L_HPLP);
26 R_LPF = filter(LPF,R_HPLP);
27
28 % construction of differentiator
29 d = firpm(3,[0 2 20 500]/500,[0 1 0 0],[1 1],'differentiator');
30 DIFF = dfilt.dffir(d);
```



```
31
32 % traveling wave signal leaving differentiator
33 - L_DIFF = filter(DIFF,L_LPF);
34 - R_DIFF = filter(DIFF,R_LPF);
35
36 % locate first peak of signal
37 - [~, timeL] = findpeaks(abs(L_DIFF),'minpeakheight',15);
38 - [~, timeR] = findpeaks(abs(R_DIFF),'minpeakheight',15);
39
40 % relate peaks to time and take the difference
41 - dpL = timeL(1);
42 - dpR = timeR(1);
43 - ta = dpL*10^(-6) - dpR*10^(-6); % difference in time of arrival
44
45 % calculate fault location
46 - fl = 0.5*(LL + ta*Vprop);
```

**Figure A-1:** MATLAB code of the TWFL.

## APPENDIX B

### IEEE 9-BUS SYSTEM PARAMETERS

The parameters of the IEEE 9-bus system are shown in the figures and tables below [10].

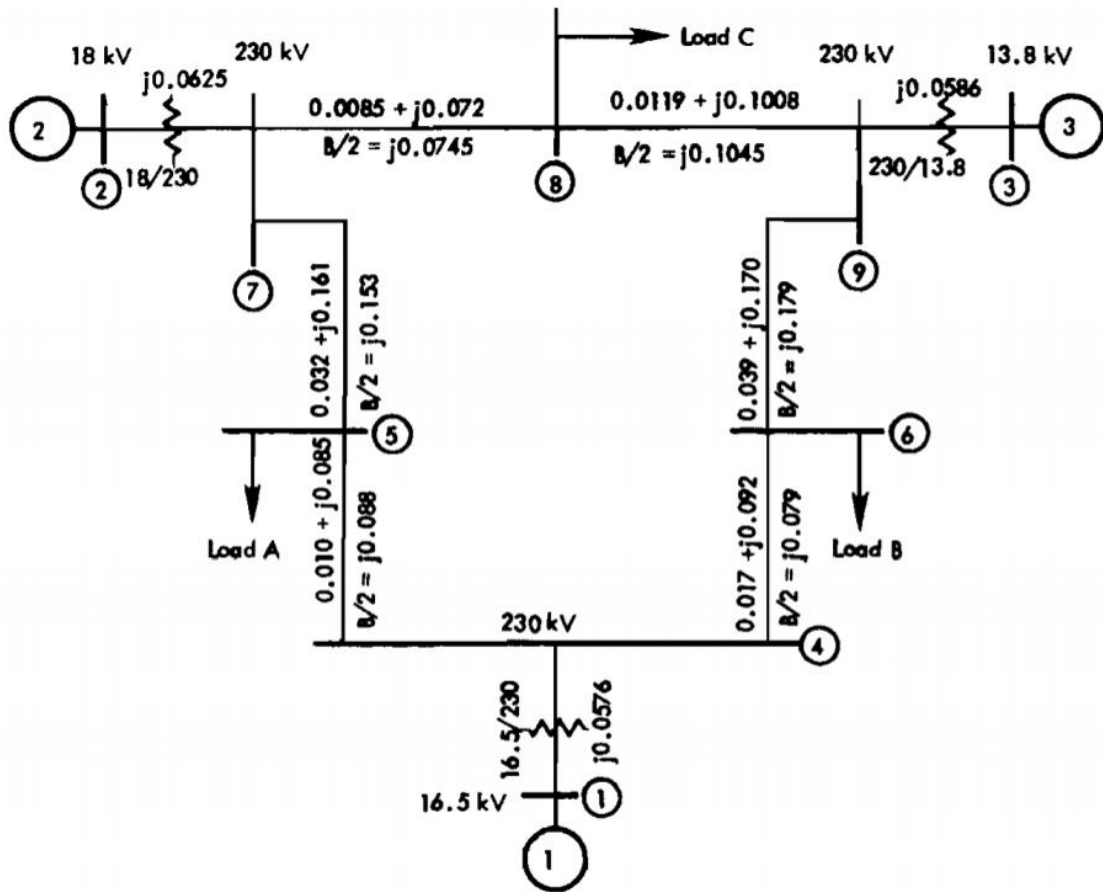


**Figure B-1:** Impedance diagram for the IEEE 9-bus system. All values are in p.u. on a 100 MVA base.

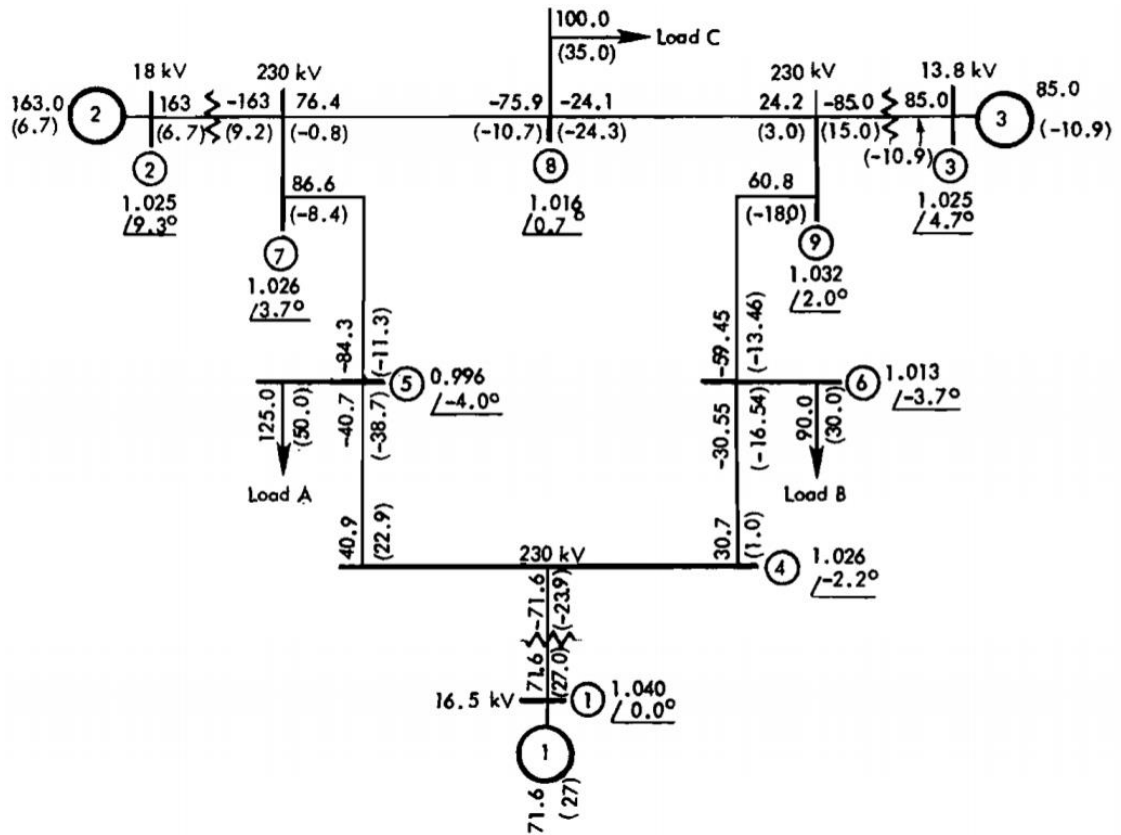


**Figure B-2:** Load flow diagram for the IEEE 9-bus system. All flows are in MW and (MVar).

**Table B-1:** Generator data for the IEEE 9-bus system.

Generator	1	2	3
Rated MVA	247.5	192	128
Rated kV	16.5	18.0	13.8
Power Factor	1.0	0.85	0.85
Type	Hydro	Steam	Steam
Speed (rpm)	180	3600	3600

## BIBLIOGRAPHY

- [1] J. L. Blackburn, *Protective Relaying: Principles and Applications*. New York: M. Dekker, 1987.
- [2] A. R. van C. Warrington, *Protective Relays: Their Theory and Practice*, 2nd ed. London: Chapman and Hall, 1969.
- [3] A. Greenwood, *Electrical Transients in Power Systems*. New York: Wiley-Interscience, 1971.
- [4] L. V. Bewley, *Traveling Waves on Transmission Systems*. New York: J. Wiley & Sons, 1933.
- [5] J. D. Glover, M. S. Sarma, and T. J. Overbye, *Power System Analysis and Design*, 5th ed. Stamford, CT: Cengage Learning, 2012.
- [6] N. Fischer, V. Skendzic, R. Moxley, and J. Needs, "Protective relay traveling wave fault location," in *11th IET International Conference on Developments in Power Systems Protection (DPSP 2012)*, 2012, p. 33.
- [7] E. O. Schweitzer, A. Guzman, M. V. Mynam, V. Skendzic, B. Kasztenny, and S. Marx, "Locating faults by the traveling waves they launch," in *40th Annual Protective Relay Conference*, 2013.
- [8] S. Marx, B. K. Johnson, A. Guzmán, V. Skendzic, and M. V Mynam, "Traveling Wave Fault Location in Protective Relays: Design, Testing, and Results," in *16th Annual Georgia Tech Fault and Disturbance Analysis Conference*, 2013.
- [9] J. Arrillaga and N. R. Watson, *Computer Modelling of Electrical Power Systems*. Chichester, UK: John Wiley & Sons, Ltd, 2001.
- [10] P. M. Anderson and A. A. Fouad, *Power System Control and Stability*. Piscataway, N.J.: IEEE Press, 2003.